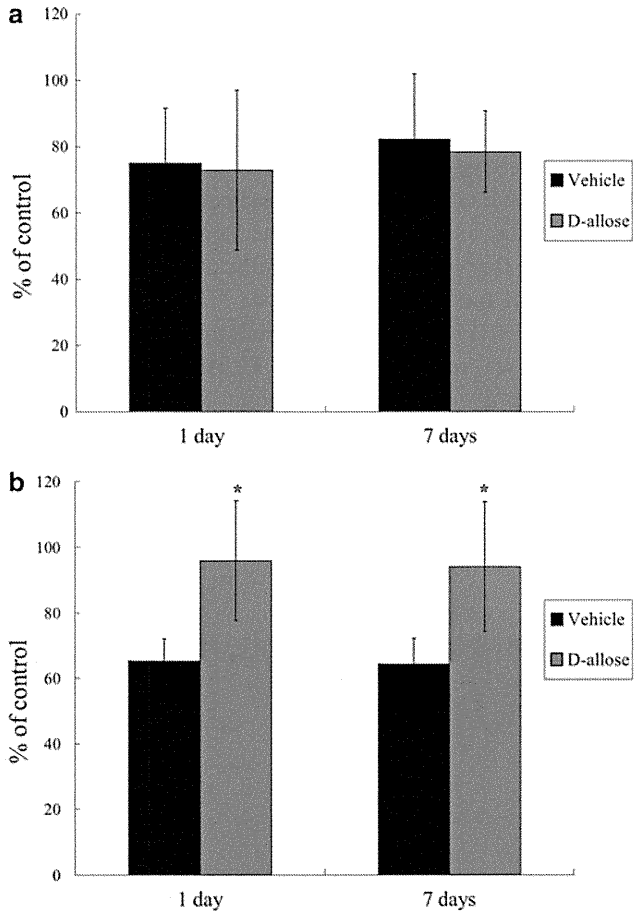

Fig. 4 **a** On postoperative day 7, the a-wave amplitude was 78.4 ± 12.3% in the D-allose group and 82.3 ± 19.6% in the vehicle group. *Gray bar* D-allose group, *black bar* vehicle group. **b** The b-wave amplitudes were 94.1 ± 19.8 and 64.3 ± 7.9%, respectively. On postoperative days 1 and 7, the mean amplitude of the b-wave for eyes treated with D-allose was significantly higher than for those treated with vehicle. *Gray bar* D-allose group, *black bar* vehicle group. Results are expressed as mean ± SD. $*P < 0.05$

Survival of RGCs

Figure 3a shows representative results of RGC labeling for both vehicle and D-allose-treated rabbits. RGC survival in the central retinas of the eyes with ischemia was 42.8 ± 8.8% in the vehicle-treated group ($n = 4$) and 81.2 ± 12.7% in the D-allose-treated group ($n = 4$, $P = 0.01$; Fig. 3b). In the peripheral retina, RGC survival in eyes with ischemia was 68.0 ± 13.8% in the vehicle-treated group and 74.7 ± 18.3% in the D-allose-treated group ($P = 0.64$; Fig. 3b).

ERGs

The mean amplitudes of both the a-wave and b-wave are shown in Fig. 4. On postoperative day 7, the a-wave amplitude was 78.4 ± 12.3% in the D-allose group ($n = 5$) and 82.3 ± 19.6% in the vehicle group ($n = 5$; Fig. 4a). The b-wave amplitudes were 94.1 ± 19.8 and 64.3 ± 7.9%, respectively (Fig. 4b). The mean amplitude of the b-wave in eyes treated with D-allose was significantly higher than in those treated with vehicle. Likewise, no significant differences in the mean amplitude of a-waves were identified between the D-allose and vehicle groups. Both a-wave and b-wave amplitudes in the non-operated eyes were stable and essentially equal both before and after surgery.

Effects of D-allose on released O_2^-

Light-microscopic photographs were taken after treatment without D-allose, i.e., BSS alone (Fig. 5a), and with D-allose (Fig. 5b). Without D-allose treatment, the blue color was observed after ischemia and became stronger over time. However, in the presence of D-allose, the blue color

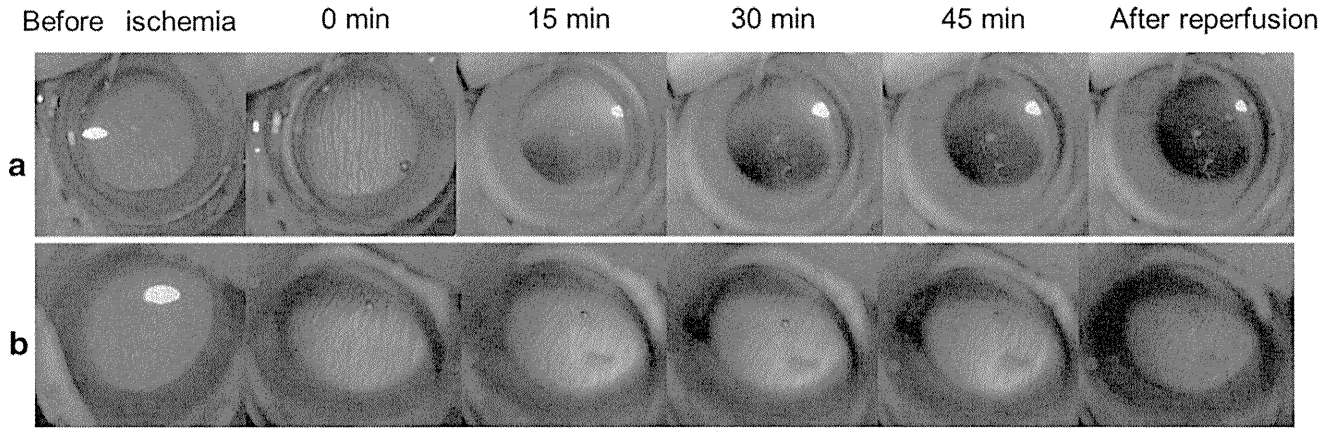

Fig. 5 Effects of D-allose on the release of superoxide anion (O_2^-). *Blue color* indicates release of O_2^-. Ischemia was induced for 45 min. Color photographs were taken before ischemia induction, then 0, 15, 30 and 45 min after starting ischemia, then immediately after reperfusion. **a** Vehicle group and **b** D-allose group

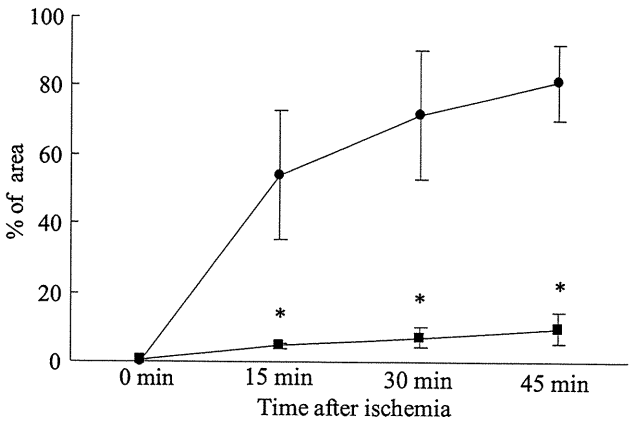

Fig. 6 Measured area O_2^- expression (%). *Filled squares* D-Allose group, *filled circles* vehicle group. Comparison of mean values of O_2^- expression between the vehicle group and the D-allose group at each time point. Mean O_2^- expression was significantly different 15, 30, and 45 min after ischemia. Data are mean ± SD. $^*P < 0.05$

decreased compared with that without D-allose. Compared with the peripheral area, the blue color intensity was stronger in the central area. Figure 6 shows results from quantification of the color levels expressed as a percentage change. Mean O_2^- expression was significantly different between the vehicle group and the D-allose group 15, 30, and 45 min after ischemia.

Discussion

These findings show that intraocular irrigation with D-allose during vitrectomy protects the morphology and function of the retina against ischemia injury.

Because D-allose may inhibit hexose transport [11], co-injection of 200 mg/kg glucose with 200 mg/kg D-allose has been shown to have no protective effect against retinal ischemia reperfusion injury [3]. BSS contains 5.11 mM glucose; i.e., approximately 0.1% glucose. Because 2% D-allose in BSS was used in this study, the glucose in BSS was not sufficient to abolish the protective effects of D-allose.

Both clinically and under experimental conditions, the functional status of the retina can be monitored continuously by recording ERGs. The b-wave of the ERG has been identified as a particularly sensitive index of retinal ischemia both in humans [12] and in experimental models of retinal ischemia in vitro [13]. Glutamate acts as a mediator of neuronal injury under ischemic conditions [14] and extracellular glutamate has been found to increase in ischemic eyes [3, 15, 16]. Reperfusion injury is thought to be mediated in part by relative hyperglycemia and high oxygen levels, leading to oxygen radical formation. D-Allose may be a down-regulation agent of hexose transport [11]. D-Allose could reduce the production of ROS by modulating the glycolytic response. Because D-allose can suppress glutamate release and the production of ROS after ischemia [3], D-allose protects both the morphology and function of the retina. Because there were no morphological changes in the outer retina in this study (data not shown), recovery of the a-wave amplitudes in the vehicle group was not suppressed. Therefore, we could not confirm any differences in the recovery of a-wave amplitudes between the vehicle and D-allose groups.

We recently reported that D-allose suppresses the production of H_2O_2 as determined by diaminobenzidine solution without hydrogen peroxide [3]. NBT is an electron acceptor that can be reduced by accepting electrons from various reductants, including superoxide [17] and other reductants, for example those generated from dehydrogenase systems [18, 19]. Studies have previously shown that NBT staining in normal rat retina is affected by inhibition of free radical-related enzyme systems, suggesting that NBT might be useful in the study of free radicals. During and after ischemic episodes, univalent reduction of oxygen in the mitochondrial respiratory chain is thought to be a major source of O_2^- [20]. O_2^- can be reduced to H_2O_2, a reaction catalyzed by superoxide dismutase (SOD) [7]. H_2O_2 has been identified as a potent inducer of apoptosis [21]. D-Allose may exert neuroprotective effects by reducing the production of not only H_2O_2, but also O_2^-.

Ocular perfusion pressure would be especially important in eyes with diabetes if, as has been suggested, autoregulation in the retina and optic nerve head is impaired [22, 23]. Because high infusion pressure during PPV is useful in preventing bleeding, we must also consider protecting the retina against damage caused by pressure-induced ischemia in cases of diabetic retinopathy [24]. Levels of glutamate potentially toxic to retinal ganglion cells have been found in the vitreous of patients with PDR [25]. This glutamate could then initiate a forward cascade of further neuronal ischemia.

Our findings suggest that intraocular irrigation with D-allose during vitrectomy may protect both the morphology and function of the retina against ischemia-induced damage.

Acknowledgments This work was supported by a Grant-in-Aid for Scientific Research from the Ministry of Education, Culture, Sports, Science, and Technology of Japan (20592078).

References

1. Bhuiyan SH, Itami Y, Yuhko R, Katayama T, Izumori K. D-Allose production from D-psicose using immobilized L-rhamnose isomerase. J Ferment Bioeng. 1998;85:540–2.
2. Murata A, Sekiya K, Watanabe Y, Yamaguchi F, Hatano N, Izumori K, et al. A novel inhibitory effect of D-allose on production of reactive oxygen species from neutrophils. J Biosci Bioeng. 2003;96:89–91.
3. Hirooka K, Miyamoto O, Jinming P, Du Y, Itano T, Baba T, et al. Neuroprotective effect of D-allose against retinal ischemia–reperfusion injury. Invest Ophthalmol Vis Sci. 2006;47:1653–7.

4. Seki M, Togashi H, Ando N. Optic nerve atrophy after vitrectomy for diabetic retinopathy: its systemic and local risk factors. Nippon Ganka Gakkai Zasshi. 2006;110:462–7.
5. Jacobson MD. Reactive oxygen species and programmed cell death. Trends Biochem Sci. 1996;21:83–6.
6. Kroemer G, Petit P, Zamzami N, Vayssière JL, Mignotte B. The biochemistry of programmed cell death. FASEB J. 1995;9:1277–87.
7. Bonne C, Muller A, Villain M. Free radicals in retinal ischemia. Gen Pharmacol. 1998;30:275–80.
8. Tamai K, Toumoto E, Majima A. Local hypothermia protects the retina from ischemic injury in vitrectomy. Br J Ophthalmol. 1997;81:789–94.
9. Traustason S, Eysteinsson T, Agnarsson BA, Stefánsson E. GABA agonists fail to protect the retina from ischemia–reperfusion injury. Exp Eye Res. 2009;88:361–6.
10. Digregorio KA, Cilento EV, Lantz RC. Measurement of superoxide release from single pulmonary alveolar macrophages. Am J Physiol. 1987;252:C677–83.
11. Ullrey DB, Kalckar HM. Search for cellular phosphorylation products of D-allose. Proc Natl Acad Sci USA. 1991;88:1504–5.
12. Coleman K, Fitzgerald D, Eustace, Bouchier-Hayes D, et al. Electroretinography, retinal ischemia and carotid artery disease. Eur J Vasc Surg. 1990;4:569–73.
13. Zager E, Ames A. Reduction of cellular energy requirements: screening for agents that may protect against CNS ischemia. J Neurosurg. 1988;69:568–79.
14. Choi DW. Glutamate neurotoxicity and diseases of the nervous system. Neuron. 1988;1:623–34.
15. Louzada-Junior P, Dias JJ, Santos WF, Lachat JJ, Bradford HF, Coutinho-Netto J. Glutamate release in experimental ischaemia of the retina: an approach using microdialysis. J Neurochem. 1992;59:358–63.
16. Adachi K, Kashii S, Masai H, Ueda M, Morizane C, Kaneda, et al. Mechanism of the pathogenesis of glutamate neurotoxicity in retinal ischemia. Graefes Arch Clin Exp Ophthalmol. 1998;236:766–74.
17. Auclair C, Voisin E. Nitroblue tetrazolium reduction. In: Greenwald RA, editor. Handbook of methods for oxygen radicals research. Boca Raton: CRC Press; 1988. p. 123–32.
18. Altman FP. Tetrazolium salts and formazans. Prog Histochem Cytochem. 1976;9:1–56.
19. Zhang H, Agardh E, Agardh CD. Nitro blue tetrazolium staining: a morphological demonstration of superoxide in the rat retina. Graefes Arch Ophthalmol. 1993;231:178–83.
20. Gonzalez-Flecha B, Boveris A. Mitochondrial sites of hydrogen peroxide production in reperfused rat kidney cortex. Biochim Biophys Acta. 1995;1243:361–6.
21. Hockenbery DM, Oltvai Z, Yin XM, Milliman CL, Korsmeyer SJ. Bcl-2 functions in an antioxidant pathway to prevent apoptosis. Cell. 1993;75:241–51.
22. Kohner EM, Patel V, Rassam SM. Role of blood flow and impaired autoregulation in the pathogenesis of diabetic retinopathy. Diabetes. 1995;44:603–6.
23. Arnold AC. Pathogenesis of nonarteritic anterior ischemic optic neuropathy. J Neuroophthalmol. 2003;23:157–63.
24. Ikushima M, Tano Y, Ikeda T, Sato Y. Hyper-infusion pressure for diabetic membrane dissection. Jpn J Ophthalmol. 1990;34:393–400.
25. Ambati J, Chalam KV, Chawla DK, D'Angio CT, Guillet EG, Rose SJ, et al. Elevated γ-aminobutyric acid, glutamate, and vascular endothelial growth factor levels in the vitreous of patients with proliferative diabetic retinopathy. Arch Ophthalmol. 1997;11:1161–6.

CORRELATION OF INCREASED FUNDUS AUTOFLUORESCENCE SIGNALS AT CLOSED MACULA WITH VISUAL PROGNOSIS AFTER SUCCESSFUL MACULAR HOLE SURGERY

CHIEKO SHIRAGAMI, MD, FUMIO SHIRAGA, MD, ERI NITTA, MD, KOUKI FUKUDA, MD, HIDETAKA YAMAJI, MD

Purpose: To study the significance of the increased fundus autofluorescence (FAF) signals at closed macula with spectral-domain optical coherence tomography and visual prognosis after successful surgery in eyes with idiopathic full-thickness macular holes (MHs).

Methods: Seventy-eight eyes of 78 consecutive patients with full-thickness MHs underwent successful standard vitrectomy, with internal limiting membrane peeling and followed by 10% sulfur hexafluoride gas injection. Simultaneous FAF and optical coherence tomography images were recorded at 10 days, and 1, 3, and 6 months postoperatively, using a combined spectral-domain optical coherence tomography–fluorescein angiography device (Spectralis™/HRA Heidelberg Retina Angiograph 2). The appearance of increased FAF in the macula postoperatively and the relationship of FAF and optical coherence tomography findings to best-corrected visual acuity were examined.

Results: Stage 2, 3, and 4 MHs were present in 31, 29, and 18 eyes, respectively. The median patient age was 66 years, with a range of 54 to 79 years. In all patients, the MHs were successfully closed, and the preoperative increased FAF corresponding to MH disappeared 10 days after surgery. In 36 eyes (46.2%), however, hyperautofluorescence again appeared in the macular area 1 month postoperatively. This hyperautofluorescence was significantly associated with the recovery of the external limiting membrane lines at the fovea 1 month after surgery ($P = 0.001$, multiple logistic regression analysis). Also, this recovery of the external limiting membrane lines 1 month postoperatively was significantly associated with the recovery of photoreceptor inner and outer segment junction line 3 months postoperatively at the fovea ($P < 0.001$, Fisher exact test). Moreover, a good best-corrected visual acuity of 20/28 or better at 6 months after surgery was significantly associated with hyperautofluorescence in the macula 1 month postoperatively, the recovery of the photoreceptor inner and outer segment lines at the fovea 3 months postoperatively, and preoperative good visual acuity ($P < 0.05$, multiple logistic regression analysis).

Conclusion: In full-thickness MHs, 46.2% of our patients showed increased FAF in the macula 1 month after successful MH surgery. This hyperautofluorescence could be a sign of good visual prognosis postoperatively.

RETINA 32:281–288, 2012

The macular hole (MH) is a full-thickness defect of the retinal tissue involving the anatomical fovea. Significant controversy still exists regarding the pathogenesis, prognosis, and management of this lesion.[1] The diagnosis of idiopathic full-thickness MHs is usually made by biomicroscopic examination and optical coherence tomography (OCT). Recently, a new technique has been developed that allows in vivo imaging of the distribution of fundus autofluorescence (FAF) using a confocal laser scanning ophthalmoscope.[2–4] In a normal fundus, the distribution of FAF is diffuse, with decreased intensity at the fovea. This technique provides high–spatial resolution imaging of the distribution of FAF, which is most

likely derived from lipofuscin within the retinal pigment epithelium (RPE).[4–9] It is generally accepted that lipofuscin represents the product of degradation of the photoreceptor outer segments. Therefore, an autofluorescent spot in the macula is consistent with a loss of the foveal tissue, especially a complete full-thickness MH. Disappearance of FAF from the MH, as may occur after successful surgical repair,[3,4] suggests that the RPE is again covered by the retinal and/or glial tissue, as demonstrated also by the OCT images.

Macular FAF is attenuated by the luteal pigment, and the concentration of this pigment in the fovea is densest along the outer plexiform layer.[10] Any foveal defect that spares the photoreceptors[11] may alter the degree of foveal FAF by decreasing the amount of masking macular pigment, therefore increasing the foveal FAF. In vivo imaging of FAF can be carried out with commercially available confocal scanning laser ophthalmoscopes.[9] Although the usefulness of this technique has already been demonstrated for the diagnosis of full-thickness MH, there are few reports[11] of postoperative increased FAF in the macula after successful MH closure. In another report, it was noted that MH closure is attained by bridge formation (foveal detachment) and healing of the photoreceptor inner and outer segment junction (IS/OS) line in varying degrees, which correlated with visual outcomes.[12,13] However, there was no discussion of the correlation between the OCT images and the FAF images of the external limiting membrane (ELM) line. As visualized on electron microscopic images, the external limiting membrane is formed by junctional complexes uniting the Muller cells to the photoreceptor cell inner segments. Therefore, the aims of this study were to investigate the significance of postoperative increased FAF in the macula and to determine the relationships among FAF findings, restoration of ELM and IS/OS line on OCT images, and best-corrected visual acuity (BCVA) after successful MH surgery.

Patients and Methods

Seventy-eight eyes of 78 consecutive patients (39 women and 39 men, ranging in age from 54 to 79 [mean, 66.0] years), who underwent vitrectomy for idiopathic MHs between April 2007 and April 2009, were included in the study. Both biomicroscopy and OCT were used to classify the MH stage. Eyes with reopened MHs, MHs with retinal detachment, MHs caused by high myopia, or other macular diseases, such as age-related macular degeneration (including dry type) combined, were excluded from this study. The study was conducted in accordance with the recommendations of the Declaration of Helsinki and was approved by the institutional review board at the Kagawa University Hospital. After an explanation of the purpose of the study and the procedures to be used, a signed informed consent was obtained from all patients before surgery and examinations.

Surgical Technique

Local anesthesia was induced by retrobulbar nerve block. A 25-gauge pars plana vitrectomy with internal limiting membrane (ILM) peeling was carried out in all eyes using the Accurus vitrectomy system (Alcon Labs, Fort Worth, TX). The posterior hyaloid was separated and removed using the 25-gauge vitreous cutter. Later, all vitreous traction on the MH was removed and the peripheral vitreous subtotally shaved. When the ILM was removed, brilliant blue G[14] was used for staining in 42 eyes, and in the other 36 eyes, triamcinolone acetonide–assisted ILM peeling was carried out. The area of ILM peeling was 2–3 optic disk diameters around the fovea. Cataract surgery combined with a vitrectomy was carried out in all 78 patients aged older than 50 years. At the end of the surgery, 10% sulfur hexafluoride gas was infused into the vitreous cavity. Face-down positioning was maintained for 3 postoperative days.

Ophthalmic Examinations and Fundus Photography

All patients underwent a regular ophthalmic examination, including measurement of the BCVA and fundus examination. Color fundus photography using the Topcon TRC-50DX fundus camera (Topcon, Tokyo, Japan) was carried out using 50° field images preoperatively and postoperatively (10 days, and 1, 3, and 6 months after the surgery in all patients). The FAF and foveal OCT images were recorded to simultaneously detect the intensity of FAF, and ELM and IS/OS line recovery using the combined spectral-domain OCT–fluorescein angiography device (Spectralis^{TM}/HRA Heidelberg Retina Angiograph 2, Heidelberg Engineering GmbH, Heidelberg, Germany) at 10 days, and 1, 3, and 6 months postoperatively. Foveal images were examined in both horizontal and in vertical directions, with averages of 100 scans using the automatic averaging and eye tracking features.

From the Department of Ophthalmology, Kagawa University Faculty of Medicine, Kagawa, Japan.

The authors have no proprietary, financial, or conflicts of interest to disclose.

Reprint requests: Chieko Shiragami, MD, Department of Ophthalmology, Kagawa University Faculty of Medicine, 1750-1 Ikenobe Miki-cho, Kagawa 761-0793, Japan; e-mail: chappi@kms.ac.jp

Statistical Methods

To determine whether there was a significant association between increased FAF at the closed MH area and several factors including patient age, preoperative BCVA, MH stage, and ELM and IS/OS line recovery at the fovea on OCT images 1 month postoperatively, multiple logistic regression analysis was carried out. The BCVA was converted to logMAR (logarithm of the minimal angle of resolution) equivalents for statistical analysis. Furthermore, factors predicting good BCVA of 20/28 or better (logMAR 0.15) at 6 months after surgery were analyzed, using patient age, increased FAF at 1 month after surgery, preoperative BCVA, IS/OS line recovery at 3 months after surgery, preoperative historical duration, MH stage, and the use of ILM staining as the factors. Also, the correlation between ELM line recovery at 1 month postoperatively and IS/OS line recovery at 3 months postoperatively was examined statistically (Fisher exact test). A P value of <0.05 was considered significant. Statistical analysis was carried out using SPSS 11.5 statistical software (SPSS, Inc, Chicago, IL).

Results

A total of 78 eyes of 78 patients with unilateral MHs were prospectively studied. Stage 2, 3 (Figure 1, 3A), and 4 MHs were present in 31, 29, and 18 eyes, respectively. Six months postoperatively, the mean logMAR visual acuity improved significantly from 0.61 ± 0.62 preoperatively to 0.17 ± 0.07 ($P < 0.001$, paired t-test). The historical duration of MHs, which corresponds to the duration since becoming aware of metamorphopsia or visual disturbance to receiving the operation in each patient, was 1 month to 15 months (mean 3.4 ± 2.1 months).

In all patients, the preoperative increased FAF corresponding to MHs (Figure 2A) disappeared 10 days after successful surgical closure. However, mild increased FAF signals at the closed macular regions were seen in 36 eyes (46.2%) at 1 month (Figure 2B), in 49 eyes (62.8%) at 3 months (Figure 2C), and in 53 eyes (67.9%) at 6 months postoperatively (Figure 2D), while there were no FAF signals in the macula (Figure 3, B–D) until 6 months postoperatively in 25 eyes (32.1%).

Fifty eyes (64.1%) had a continuous ELM line on the foveal OCT images, which corresponds to ELM recovery 1 month after surgery (Figure 2B), whereas in 42 eyes, the ELM line showed a defect (Figure 3B), which indicates that the ELM had not recovered. Continuous ELM lines on OCT images were seen in 67 eyes (85.9%) at 3 months (Figures 2C, 3C) and in 76 eyes (97.4%) at 6 months (Figures 2D, 3D) after surgery.

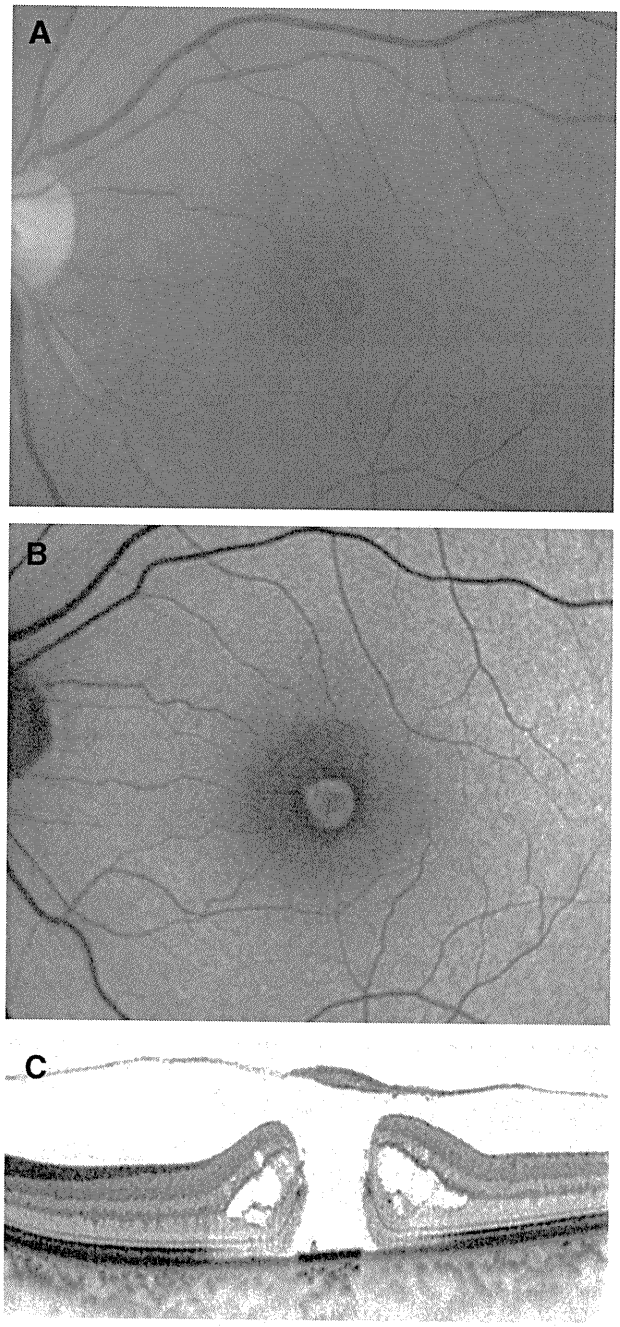

Fig. 1. Case 1. A 70-year-old man with a stage 3 MH in his left eye. **A.** The preoperative visual acuity was 20/50. The preoperative color photograph indicates MH with a surrounding fluid cuff. **B.** The FAF image taken preoperatively demonstrates increased FAF corresponding to the defect of the neurosensory retina. **C.** The optical coherence tomographic image taken preoperatively.

In contrast, only 6 of the 78 eyes (7.7%) had the continuous IS/OS line (Figures 2B, 3B) at 1 month postoperatively. The continuous IS/OS line recovery on OCT images was seen in 41 eyes (52.6%) at

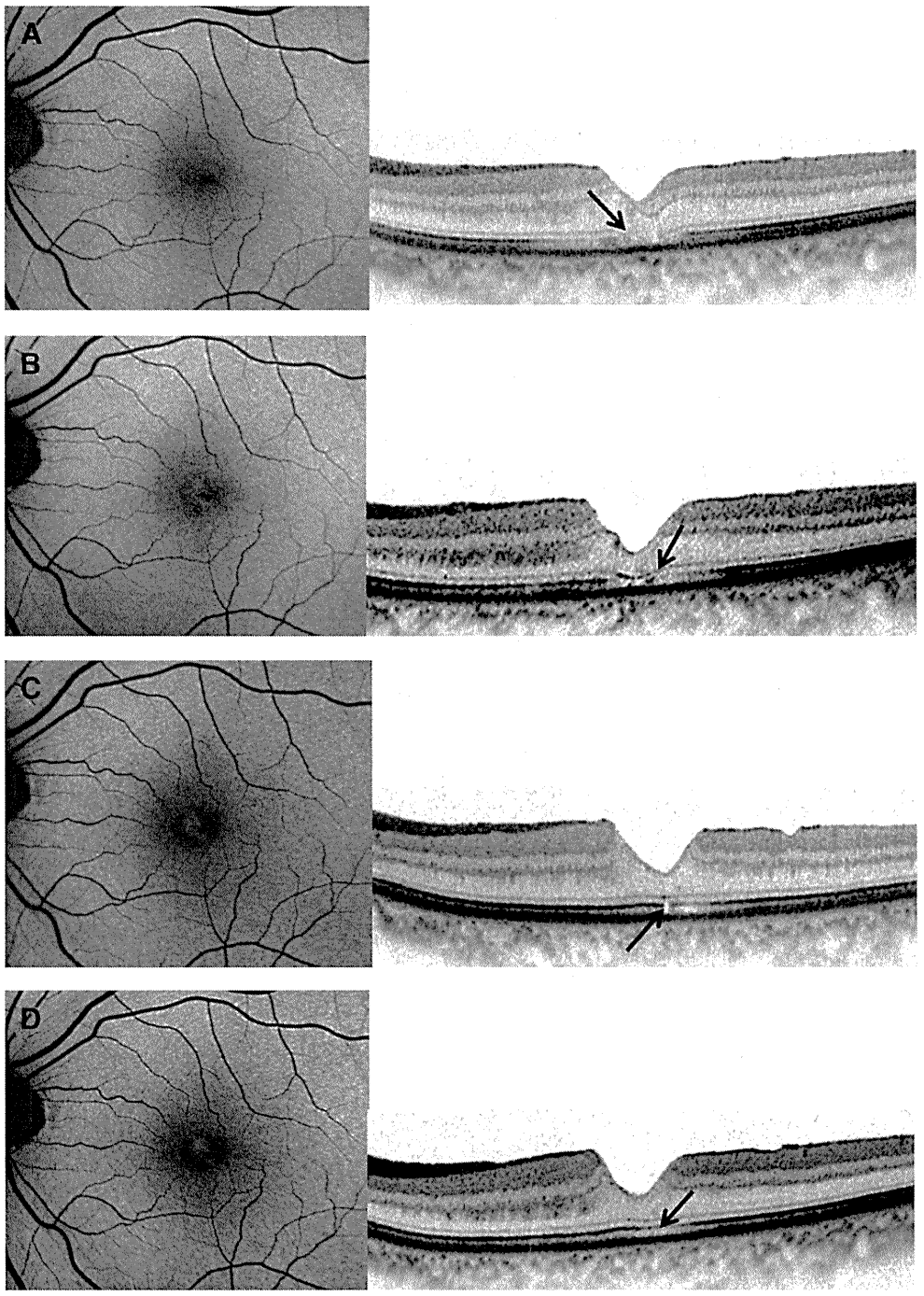

Fig. 2. The postoperative FAF images and OCT in Case 1. **A.** The FAF image (left) and OCT (right) taken 10 days postoperatively. The FAF demonstrates a decreased FAF signal at the closed macular area, and an outer foveal defect with disrupted ELM line and IS/OS line remains (arrow). **B.** FAF image taken 1 month postoperatively demonstrates a mild increased FAF signal at the closed MH (left). The OCT taken 1 month postoperatively shows a continuous ELM line (arrow), although an IS/OS line is disrupted (right), and the BCVA was increased to 20/22. **C.** FAF image taken 3 months postoperatively demonstrates the increased FAF signal at the closed MH (left). The OCT taken 3 months postoperatively shows a continuous ELM line and an IS/OS line with a minimal defect (right; arrow), and the BCVA was 20/20. **D.** FAF image taken 6 months postoperatively is almost the same as the FAF in the left panel. The OCT taken 6 months postoperatively shows a continuous ELM line and a continuous IS/OS line (right; arrow), and the BCVA was 20/20.

3 months (Figure 2C) and in 65 eyes (83.3%) at 6 months (Figure 2D) postoperatively.

In 25 patients whose macula continued showing hypoautofluorescence during observation 6 months after surgery (Figure 3), ELM line recovery was seen in only 8 eyes and IS/OS line recovery in only 1 eye 1 month after surgery. Eventually, in these cases of hypoautofluorescence in the macula, the recovery of ELM and IS/OS lines was seen in 20 eyes (80%) and 18 eyes (72%), respectively, 6 months postoperatively. It was obvious that, in cases of a hypoautofluorescent macula on FAF images, morphologic recovery of ELM and IS/OS lines was delayed, compared with the cases of hyperautofluorescent macula (Figure 3, B–D).

In all patients, the inner retinal layer, such as the inner nuclear layer, and the inner and outer plexiform layers, recovered with time. After 1 month to 3 months after the MH surgery, the structure of the inner retinal

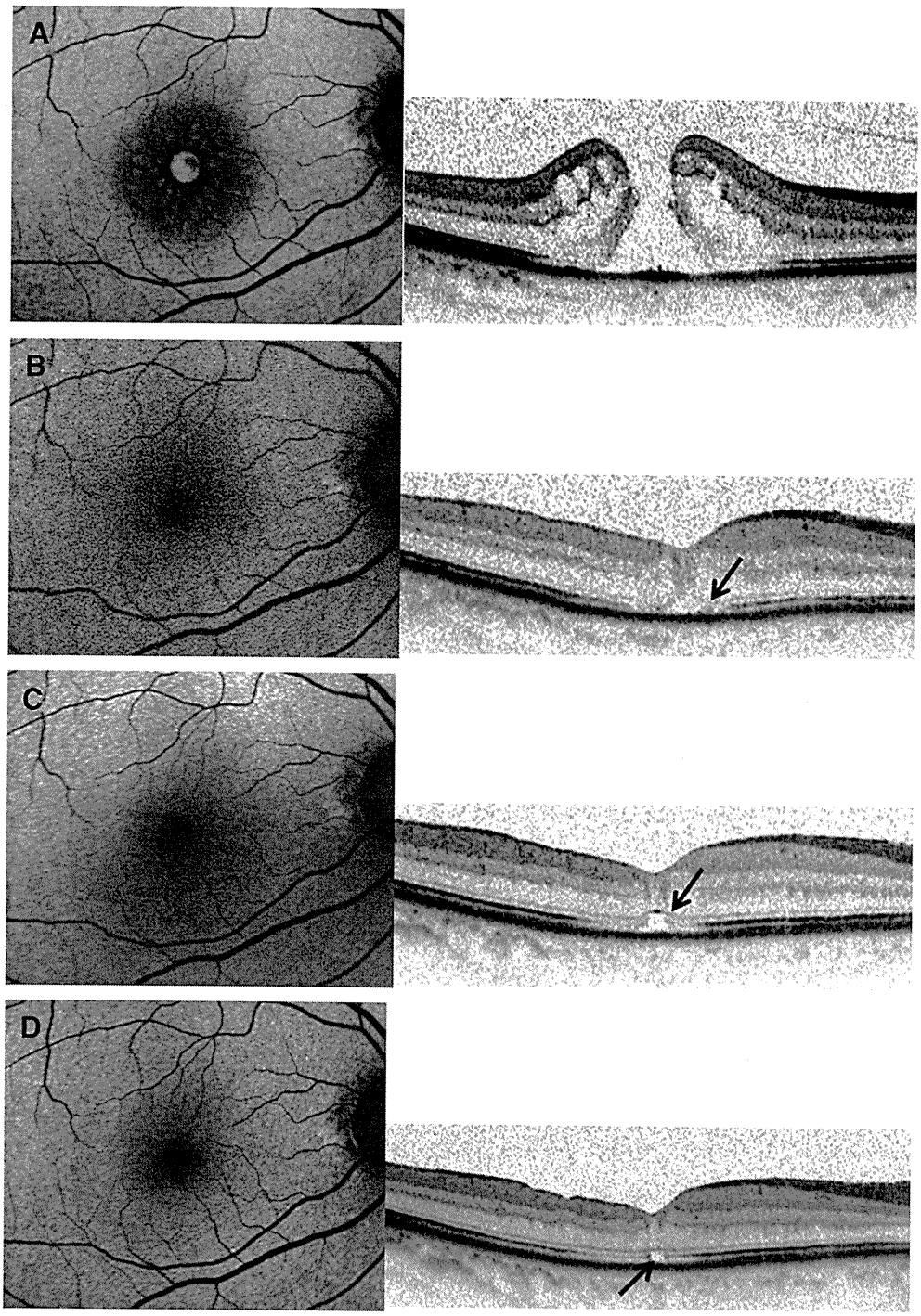

Fig. 3. Case 2. A 71-year-old woman with a stage 3 MH in her right eye. **A.** The preoperative BCVA was 20/50. The FAF image (left) taken preoperatively demonstrates increased FAF corresponding to the defect of the neurosensory retina (right). **B.** The FAF image taken 1 month postoperatively demonstrates hypofluorescence in the macula (left). The OCT taken 1 month postoperatively shows a disrupted ELM line (arrow) and a disrupted IS/OS line (right), and the BCVA remains 20/50. **C.** FAF image taken 3 months postoperatively demonstrates hypofluorescence in the macula (left). The OCT taken 3 months postoperatively shows a continuous ELM line (arrow) and foveal detachment with a disrupted IS/OS line (right). **D.** FAF image taken 6 months postoperatively still demonstrates hypofluorescence in the macula (left). The disruption of the IS/OS line (arrow) remains 6 months postoperatively (right). The BCVA was not improved.

layer appeared quite normal on the OCT images (Figures 2B, 3C).

Changes in the logMAR BCVA at 6 months postoperatively showed significant differences between the ELM recovery group and ELM nonrecovery group 1 month postoperatively (Student *t*-test, $P < 0.001$; Figure 4). Although, the features of the outer photoreceptor layer on the OCT images showed that the ELM lines recovered earlier than the IS/OS lines in the eyes of all patients, the IS/OS line recovery at 3 months postoperatively was significantly correlated with the ELM recovery at 1 month postoperatively ($P < 0.001$).

The appearance of increased FAF signals 1 month postoperatively was significantly associated with the ELM recovery at the fovea 1 month postoperatively

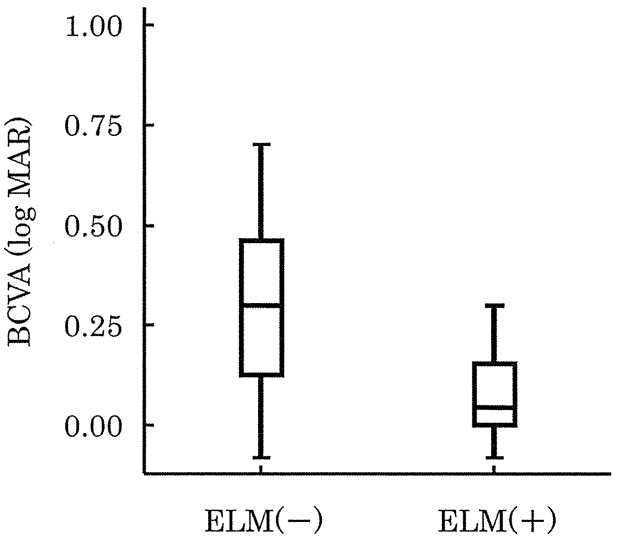

Fig. 4. Box plots showing BCVA 6 months after MH surgery in the group in which ELM recovery was not present 1 month after surgery (ELM−) and in the group with early ELM recovery 1 month after surgery (ELM+). The boxes show the median (line) and 25th and 75th percentiles. LogMAR, logarithm of the minimal angle of resolution.

(P = 0.001; Table 1). Moreover, good BCVA of 20/28 or better 6 months after the surgery was significantly associated with increased macular FAF 1 month postoperatively (P = 0.003), good preoperative visual acuity (P = 0.007), and IS/OS line recovery at the fovea 3 month postoperatively (P = 0.029; Table 2).

Discussion

Fundus autofluorescence imaging using a confocal scanning laser ophthalmoscope derives from the lipofuscin-laden RPE.[4,9] The autofluorescence is attenuated by the luteal pigment in the macula. Therefore, an autofluorescent spot in the macula is consistent with a loss of the foveal tissue, either partial (lamellar MH) or complete full-thickness MH.[4] Disappearance of FAF from the MH, as occurs after successful surgical repair,[3,4] suggests that, in our case, the RPE was again covered by the retinal and/or glial tissue, as demonstrated also by the OCT images. In our study, the completely closed MH after successful surgical treatment showed disappearance of autofluorescence 10 days postoperatively, similar to the normal fundus. In the eyes of almost half of the total number of patients (46.2%), closed macular areas again showed mildly increased FAF signals 1 month after surgery. Whereas the appearance of increased FAF signals 1 month postoperatively was significantly associated with early ELM recovery at the fovea 1 month postoperatively, postoperative good BCVA of 20/28 or better 6 months after MH closure was significantly associated with increased FAF, preoperative BCVA, and IS/OS recovery at 3 months postoperatively. Also, these results indicate that this increased FAF signal may predict a good visual prognosis after MH surgery. Early ELM recovery at the fovea 1 month postoperatively was significantly associated with IS/OS recovery 3 months postoperatively. The reason why the closed MH area shows an increased FAF signal is however unclear.

Generally, in normal eyes, macular pigment, which is composed of lutein and zeaxanthin, is important for the maintenance of macular health through its absorptive and/or antioxidant properties.[15–18] These compounds are especially dense in the axons of cone photoreceptors at the fovea, although cells in the inner nuclear layer and the inner and outer plexiform layers also contain these compounds.[15–18] After successful MH closure, the structure of the retinal layer in the macula may not recover completely. Hangai et al[19] reported that centrifugal enlargement of tiny interruptions in the ELM occurs in an MH if the Muller cell cone is dragged away. Their report proved that there is less of a defect in the tissue in MH but rather centrifugal displacement of the photoreceptors occurs. Because

Table 1. Multiple Logistic Regression Model of Variables Associated with Increased FAF 1 Month After MH Closure

	Odds Ratio	95% CI	P
Age	0.971	0.906–1.041	0.405
ELM line recovery*	8.230	2.441–27.750	0.001
IS/OS line recovery*	1.588	0.246–10.259	0.627
Preoperative BCVA	0.514	0.034–7.758	0.631
Stage	1.221	0.634–2.354	0.550

CI, confidence interval.
*1 month after MH surgery.

Table 2. Multiple Logistic Regression Model of Variables Associated with Postoperative Good Visual Acuity 6 Months After MH Closure

	Odds Ratio	95% CI	P
Age	0.976	0.898–1.060	0.563
Increased FAF*	7.376	1.986–27.397	0.003
Preoperative BCVA	192.398	4.313–8583.242	0.007
IS/OS line recovery†	4.181	1.154–15.153	0.029
Preoperative historical duration	0.725	0.521–1.008	0.056
Stage	0.772	0.348–1.713	0.525
ILM staining	1.934	0.563–6.640	0.295

*1 months after MH surgery.
†3 months after MH surgery.

ELM is a part of Muller cells, early ELM recovery might indicate early recovery of the retinal morphologic structure, including inner retinal layers. The ELM lines recovered earlier than the IS/OS lines in the eyes of all patients, and the IS/OS line recovery at 3 months postoperatively was significantly correlated with the ELM recovery at 1 month postoperatively. Moreover, the continuous IS/OS line recovery at the fovea 3 months postoperatively is significantly associated with a good visual prognosis 6 months postoperatively. Briefly, the presence of a normal IS/OS line may indicate morphologic and functional recovery of the photoreceptors.[17] In our study, the increased FAF signal 1 month postoperatively, which was almost absent 10 days postoperatively, was significantly associated with early ELM recovery. The factors influencing this increase in the eyes that had early ELM recovery resulting in a good visual prognosis may include the morphologic changes of the inner retinal layers, for example, lateral displacement of the inner retinal layers with time (Figure 2). It is hypothesized that if displacement of the macular pigment–containing inner retinal layers exists at the fovea soon after the surgery and if the RPE function is normal at the macular area, the hyperautofluorescence may be concealed by the macular pigment. Later, the inner retinal layers move to the normal position with time and the hyperautofluorescence can be seen through the damaged macula with decreasing pigment concentration after the surgery. In this study, 46.2% eyes showed hyperautofluorescence at the macular area 1 month postoperatively. This result indicates that, in those eyes, hyperautofluorescence was caused by both the decreased macular pigment and the RPE that had normal metabolic function.

In contrast, late ELM recovery indicates insufficient recovery of the retinal structure leading to late IS/OS recovery resulting in photoreceptor dysfunction at the fovea after MH surgery. In the human RPE, lipofuscin accumulates as a by-product of phagocytosis of the photoreceptor outer segments. Fundus autofluorescence in the RPE depends on the outer segment renewal and is potentially affected by a balance between accumulation and clearance. So, the late IS/OS line recovery might be the reason for decreased FAF signals at closed macula after surgery; in other words, the disappearance of FAF as a surrogate marker for monitoring the functional recovery of the photoreceptors and the restoration of RPE–photoreceptor interactions in repaired MH, the complete disappearance of increased FAF and a loss of pigment or RPE death, respectively.

Another possible concern regarding the disappearance of FAF as a surrogate speculated that the restoration of hypoautofluorescence in the fovea after MH surgery could not be achieved without recovery of the inner retinal layer. Simply extending neurosensory retinal or glial tissues over the bare RPE after MH surgery would not result in complete disappearance of FAF. Improved visual acuity of patients with repaired MHs obviously implies that the photoreceptor function is recovered, both morphologically and functionally. The interpretation of FAF in repaired MH could be complicated because it might also be influenced by other cells and tissues in the fovea as a result of their minor contributions to the macular pigment.

In this study, the historical duration of MH was not significantly associated with visual prognosis but tended to be correlated with good visual prognosis ($P = 0.056$; Table 2) This shows that, in chronic MH, once the bare RPE is surgically covered with neurosensory retinal tissue, normal interactions between the RPE and the photoreceptors may be slightly difficult.

In conclusion, increased FAF early after MH surgery is an important indicator of ELM recovery leading to the early recovery of photoreceptors, predicting a good postoperative visual prognosis. This increased FAF signal may be induced by normal metabolic activity of the RPE cells along with normal photoreceptor recovery. Further careful investigation and long-term follow-up of these patients are required to better understand the usefulness of FAF after MH surgery.

Key words: fundus autofluorescence, external limiting membrane, idiopathic full-thickness macular hole, spectral-domain optical coherence tomography.

References

1. Gass JDM. Reappraisal of biomicroscopic classification of stages of development of a macular hole. Am J Ophthalmol 1995;119:752–759.
2. Milani P, Seidenari P, Carmassi L, Bottoni F. Spontaneous resolution of a full thickness idiopathic macular hole: fundus autofluorescence and OCT imaging. Graefes Arch Clin Exp Ophthalmol 2007;245:1229–1231.
3. Ciardella AP, Lee GC, Langton K, et al. Autofluorescence as a novel approach to diagnosing macular holes. Am J Ophthalmol 2004;137:956–959.
4. von Rückmann A, Fitzke FW, Gregor ZJ, Fundus autofluorescence in patients with macular holes imaged with a laser scanning ophthalmoscope. Br J Ophthalmol 1998;82: 346–351.
5. Spaide RF. Autofluorescence from the outer retina and subretinal space: hypothesis and review. Retina 2008;28:5–35.

6. Spaide RF. Fundus autofluorescence and age-related macular degeneration. Ophthalmology 2003;110:392–399.
7. Chung JE, Spaide RF. Fundus autofluorescence and vitelliform macular dystrophy. Arch Ophthalmol 2004;122:1078–1079.
8. Schmitz-Valckenberg S, Holz FG, Bird AC, Spaide RF. Fundus autofluorescence imaging: review and perspectives. Retina 2008;28:385–409.
9. Delori FC, Dorey CK, Staurenghi G, et al. In vivo fluorescence of the ocular fundus exhibits retinal pigment epithelium lipofuscin characteristics. Invest Ophthalmol Vis Sci 1995;36:718–729.
10. Snodderly DM, Auran JD, Delori FC. The macular pigment. II. Spatial distribution in primate retinas. Invest Ophthalmol Vis Sci 1984;25:674–685.
11. Chung H, Shin CJ, Kim JG, et al. Correlation of microperimetry with fundus autofluorescence and spectral-domain optical coherence tomography in repaired macular holes. Am J Ophthalmol 2011;151:128–136.
12. Inoue M, Watanabe Y, Arakawa A, et al. Spectral-domain optical coherence tomography images of inner/outer segment junctions and macular hole surgery outcomes. Graefes Arch Clin Exp Ophthalmol 2009;247:325–330.
13. Sano M, Shimoda U, Hashimoto H, Kishi S. Restored photoreceptor outer segment and visual recovery after macular hole closure. Am J Ophthalmol 2009;147:313–318.
14. Enaida H, Hisatomi T, Hata Y, et al. Brilliant blue G selectively stains the internal limiting membrane/brilliant blue G-assisted membrane peeling. Retina 2006;26:631–636.
15. Neelam K, O'Gorman N, Nolan J, et al. Macular pigment levels following successful macular hole surgery. Br J Ophthalmol 2005;89:1105–1108.
16. Beatty S, Boulton ME, Henson DB, et al. Macular pigment and age related macular degeneration. Br J Ophthalmol 1999;83:867–877.
17. Davies NP, Morland AB. Macular pigments: their characteristics and putative role [review]. Prog Retin Eye Res 2004;23:533–559.
18. Schütt F, Davies S, Kopitz J, et al. Photodamage to human RPE cells by A2-E, a retinoid component of lipofuscin. Invest Ophthalmol Vis Sci 2000;41:2303–2308.
19. Hangai M, Ojima Y, Gotoh N, et al. Three-dimensional imaging of macular holes with high-speed optical coherence tomography. Ophthalmology 2007;114:763–773.

Current Eye Research, 36(11), 1037–1046, 2011

ISSN: 0271-3683 print/ 1460-2202 online
DOI: 10.3109/02713683.2011.594201

informa
healthcare

ORIGINAL ARTICLE

Deleterious Role of Anti-high Mobility Group Box 1 Monoclonal Antibody in Retinal Ischemia-reperfusion Injury

Shenyang Yang[1,3], Kazuyuki Hirooka[1], Ye Liu[1,5], Tomoyoshi Fujita[1], Kouki Fukuda[1], Takehiro Nakamutra[2], Toshifumi Itano[2], Jiyong Zhang[4], Masahiro Nishibori[4], and Fumio Shiraga[1]

[1]Department of Ophthalmology, Kagawa University Faculty of Medicine, Kagawa, Japan, [2]Department of Neurobiology, Kagawa University Faculty of Medicine, Kagawa, Japan, [3]Department of Ophthalmology, Shengjing Affiliated Hospital, China Medical University, Shenyang, China, [4]Department of Pharmacology, Okayama University Graduate School of Medicine, Density and Pharmaceutical Sciences, Okayama, Japan, and [5]Department of Ophthalmology, The Fourth Affiliated Hospital, China Medical University, Shenyang, China

ABSTRACT

Purpose: To investigate the effect of anti-high mobility group box 1 (HMGB1) monoclonal antibody (mAb) against ischemia-reperfusion injury in the rat retina.

Materials and Methods: Retinal ischemia was induced by increasing and then maintaining intraocular pressure at 130 mmHg for 45 min. An intraperitoneal injection of anti-HMGB1 mAb was administered 30 min before ischemia. Retinal damage was evaluated at 7 days after the ischemia. Immunohistochemistry and image analysis were used to measure changes in the levels of reactive oxygen species (ROS) and the localization of anti-HMGB1 mAb. Dark-adapted full-field electroretinography (ERG) was also performed.

Results: Pretreatment with anti-HMGB1 mAb significantly enhanced the ischemic injury of the retina. HMGB1 expression increased at 6–12 h after ischemia in the retina. After the ischemia, production of ROS was detected in retinal cells. However, pretreatment with anti-HMGB1 mAb increased the production of ROS. On the seventh postoperative day, the amplitudes of both the ERG a- and b-waves were significantly higher in the vehicle group than in the groups pretreated with anti-HMGB1 mAb.

Conclusions: The current *in vivo* model of retinal injury demonstrated that anti-HMGB1 mAb plays a large deleterious role in ischemia-reperfusion injury. In order to develop neuroprotective therapeutic strategies for acute retinal ischemic disorders, further studies on anti-HMGB1 mAb function are needed.

Keywords: Anti-HMGB1 mAb, Retinal ischemia, Reactive oxygen species, Electroretinogram, Retinal thickness

INTRODUCTION

Ischemic injury to the retina is a major cause of visual loss and morbidity. As these morbidities are difficult to treat, research into various potential treatments is currently ongoing.[1–5] Ischemia-reperfusion injury involves many signaling mechanisms that ultimately result in necrotic and apoptotic cell death.[6] Delayed neuronal cell death in the brain and retina secondary to transient ischemic injury occurs, in part, by apoptosis.[7,8] During or after ischemia, reactive oxygen species (ROS) can be produced in large quantities and act as cytotoxic metabolites.[9] ROS can provoke cell death by reacting with cell components that lead to necrosis, or by activating specific targets that trigger apoptosis.

High-mobility group box-1 (HMGB1) protein was originally described 30 years ago as a nonhistone DNA-binding protein with high-electrophoretic mobility.[10] HMGB1 is a nuclear protein involved in nucleosome stabilization and gene transcription.[11] It is known that these functions are essential for survival, as HMGB1-deficient mice have been shown to die of hypoglycemia within 24 h of birth.[12] HMGB1 is

Received 19 November 2010; accepted 31 May 2011

Correspondence: Kazuyuki Hirooka, MD, PhD, Department of Ophthalmology, Kagawa University Faculty of Medicine, 1750-1 Ikenobe, Miki, Kagawa 761-0793 Japan. Tel: +81 87 891 2211. Fax: +81 87 891 2212. E-mail: kazuyk@med.kagawa-u.ac.jp

found in almost all eukaryotic cells, and its presence has been confirmed in the rodent retina.[13] HMGB1 has also been implicated in the mechanism of ischemic brain damage.[14–20] In a stroke model, short hairpin (sh) RNA-mediated HMGB1 down-regulation in the brain reduces the severity of lesions.[15] Intravenous injection of the anti-HMGB1 monoclonal antibody (mAb) causes a dramatic reduction in the infarct size in the stroke model.[17]

The purpose of the present study was to investigate the role of anti-HMGB1 and its specific expression in retinal ischemia-reperfusion injury.

MATERIAL AND METHODS

Animals

Male Sprague-Dawley rats weighing 200–250 g were obtained from Charles River Japan (Yokohama, Japan). Rats were permitted free access to standard rat food (Oriental Yeast Co., Ltd., Tokyo, Japan) and tap water. Animal care and all experiments were conducted in accordance with the approved standard guidelines for animal experimentation of the Kagawa University Faculty of Medicine, and adhered to the ARVO Statement for the Use of Animals in Ophthalmic and Vision Research. Anti-HMGB mAb or IgG2a was injected by three different methods. Intraperitoneal injection of anti-HMGB1 monoclonal antibody (mAb) (200 μg)[17] or class-matched control mAb (IgG2a) (200 μg) against *Keyhole Limpet* hemocyanin was administered 30 min before ischemia. Anti-HMGB mAb (200 μg) or IgG2a (200 μg) was administered intravenously immediately and 6 h after reperfusion. The pupil was dilated with topical phenylephrine hydrochloride and tropicamide; anti-HMGB mAb (20 μg) or IgG2a (20 μg) was injected into the vitreous space 30 min before ischemia.

Ischemia

Rats were anesthetized by an intraperitoneal injection of 50 mg/kg pentobarbital sodium (Abbott, Abbott Park, IL) followed by a topical administration of 0.4% oxybuprocaine hydrochloride. The anterior chamber of the right eye was cannulated with a 27-gauge infusion needle connected to a reservoir containing normal saline. The intraocular pressure (IOP) was raised to 130 mmHg for 45 min by elevating the saline reservoir. Only the right eye of each rat was subjected to ischemia. Retinal ischemia was indicated by whitening of the iris and fundus. The left eyes served as the sham-treated controls, with these eyes undergoing a similar procedure that did not include elevation of the saline bag, thus maintaining normal ocular tension. Rectal and tympanic temperatures were maintained during the operation at approximately 37°C via the use of a feedback-controlled heating pad (BRC, Nagoya, Japan). After restoration of blood flow, temperature was maintained continuously at 37°C.

HISTOLOGICAL EXAMINATION

For histological examination, rats were anesthetized by intraperitoneal injection of pentobarbital sodium (50 mg/kg) 7 days after ischemia. Eyes were enucleated and stored in a 4% paraformaldehyde solution for 24 h at room temperature. The retinas were removed and embedded in paraffin, and thin sections (5-μm thickness) were cut using a microtome. Each retina was mounted on a silane-coated glass slide and then stained with hematoxylin and eosin (HE).

Morphometric analysis was performed to quantify ischemic injury. These sections were selected randomly in each eye. Light microscopic examination was performed by a person with no prior knowledge of the treatments. A microscopic image of sections obtained within 0.5–1 mm of the optic disc was scanned. For each computer image, the number of cells in the ganglion cell layer (GCL) was counted. The thicknesses of the inner plexiform layer (IPL), inner nuclear layer (INL), outer nuclear layer (ONL), and outer plexiform layer (OPL) for the entire frame were measured. The number of cells in the GCL was normalized as linear cell density (cells per millimeter). Thicknesses of the IPL, INL, ONL, and OPL were obtained by calculating the mean value of seven measurements in each eye. Similarly, the linear cell density in the GCL was also determined by calculating the mean value of seven measurements. For each animal, the right eye parameter was normalized to that of the intact left eye and shown as a percentage.

ELECTRORETINOGRAMS (ERGS)

ERG responses were measured after overnight dark adaptation (at least 6 h) using a recording device (Mayo Corporation, Aichi, Japan) 7 days after ischemia. Rats were anesthetized by an intraperitoneal injection of 50 mg/kg pentobarbital sodium. Pupils were dilated with 0.5% tropicamide and 0.5% phenylephrine hydrochloride eye drops (Santen Pharmaceuticals, Osaka, Japan). All procedures were performed in dim red light, with all rats kept warm during the procedure. The LED corneal electrode was set vertical to the cornea center. A reference electrode was set subcutaneously on the forehead and the ground connection was set on the base of the tail. An LED stimulator LS-W controlled the stimulus duration and intensity during the 11-step intensity series, which ranged from 0.0003–30 cds/m^2. The ERG response was amplified using an AC amplifier ML135 (Bio Amplifier, AD Instruments, NSW, Australia) with a bandwidth of 0.3–500 Hz and amplification of 2,000 times. The ischemic damage to the retina was

evaluated as the percentage of the a- and b-wave amplitudes of the ischemic right eyes as compared to the non-ischemic left eyes.

IMMUNOHISTOCHEMISTRY

Eyes were enucleated at 6, 12 or 24 h after 45 min of ischemia. Eyes were then fixed in 4% paraformaldehyde in the PBS and embedded in paraffin. Retinal sections (5 μm) were rinsed in 100% ethanol twice for 5 min each, followed by a separate 95% ethanol and 90% ethanol rinse for 3 min each. The sections were then washed using PBS, pH 7.4, three times for 10 min each and treated with 0.3% Triton X-100 in PBS, pH 7.4, for 1 h. After further washing three times for 10 min each with PBS, pH 7.4, sections were then blocked in 3% normal horse serum and 1% bovine serum albumin (BSA) in PBS for 1 h in order to reduce nonspecific labeling. Sections were incubated overnight at 4°C in PBS with either 2.0 mg/mL of monoclonal antibody against HMGB1[17] which served as the primary antibody. After washing in PBS for 50 min, sections were then immersed in the second antibody conjugated to horseradish peroxidase for 1 h at room temperature. Images were acquired using 40× objective lenses (DXM 1200; Nikon, Tokyo, Japan). Adobe PhotoShop v. 5.0 was used to adjust the brightness and contrast of the images.

FLUORESCENT LABELING OF ROS

To investigate the production of ROS, we intraperitoneally injected 5 mg/kg dihydroethidium (DHE; Sigma-Aldrich, St. Louis, MO) in 5% dimethyl sulfoxide (DMSO) in PBS 15 min before ischemia. A 0.3-mL aliquot of distilled water, 200 μg anti-HMGB1 mAb, or 200 μg IgG2a was administered intraperitoneally 30 min before ischemia. Eyes were enucleated 15 min after ischemia and then embedded in OCT compound (Sakura Finetek, Torrance, CA), after which cryosections (20 μm) were prepared. Sections were examined with a microscope (Radiance 2100/Rainbow, Carl Zeiss, München, Germany) using a laser set (excitation laser 514 nm; emission laser >580 nm).

Statistical Analysis

Fluorescence was quantified by automated image analysis with Image-Pro Plus software (version 4.0, Media Cybernetics, The Imaging Expert, Bethesda, MD). For each section, mean fluorescence was calculated from five separate high-power fields per eye. A threshold was set to define positive labeling.

All data are presented as the mean ± SD. Data were analyzed using an independent Student's *t*-test and ANOVA followed by Tukey-Kramer post-hoc testing corrected for multiple comparisons. Statistical analysis was performed using SPSS for Windows (SPSS Inc, Chicago, IL). A p value of < 0.05 was considered statistically significant.

RESULTS

Histologic Changes in the Retina after Ischemia with Anti-HMGB1

Figure 1A shows a normal retina. Light microscopic photographs were taken 7 days after ischemia and treatment with IgG2a (Figure 1B) or anti-HMGB1 (Figure 1C). In animals pretreated with IgG2a, the GCL cell number was reduced to 73.9 ± 16.2% of the control; the IPL thickness was reduced to 67.7 ± 14.6% of the control; the INL thickness was reduced to 82.8 ± 13.5% of the control; the OPL thickness was reduced to 88.6 ± 30.8% of the control; and the ONL thickness was reduced to 88.1 ± 13.0% of the control ($n=7$; Figure 1D). In animals pretreated with anti-HMGB1 mAb, the GCL cell numbers were 67.7 ± 16.8% of the control ($p=0.50$); the IPL thickness was 51.6 ± 12.3% of the control ($p=0.02$); the INL thickness was 69.0 ± 6.8% of the control ($p=0.03$); the OPL thickness was 51.9 ± 10.8% of the control ($p=0.01$); and the ONL thickness was 72.4 ± 13.7% of the control ($p=0.049$) ($n=7$; Figure 1D).

Treatment with intravenous injection of IgG2a or anti-HMGB1 mAb twice (immediately and 6 h after reperfusion) reduced the retinal thickness dramatically (n = 4, each group) (Figure 2).

Treatment with local administration of IgG2a or anti-HMGB1 mAb 30 min before ischemia was similar to the results with intraperitoneal injection of anti-HMGB1 mAb ($n=4$, each group) (Figure 3).

EFFECT OF ANTI-HMGB1 ON NORMAL RETINA

Animals were killed at 7 days after the intraperitoneal injection of anti-HMGB1 mAb or IgG2a. Treatment with anti-HMGB1 did not affect the retinal thickness in normal rat (Figure 4) ($n=4$, each group).

EFFECT OF ANTI-HMGB1 ON RETINAL FUNCTION

Scotopic ERG was recorded to evaluate anti-HMGB1 mAb effects on retinal function. A representative example of function is seen in Figure 5A. Mean amplitudes of the a- and b-wave are shown in Figure 5B. We observed a statistically significant difference between the three groups ($n=5$, each group).

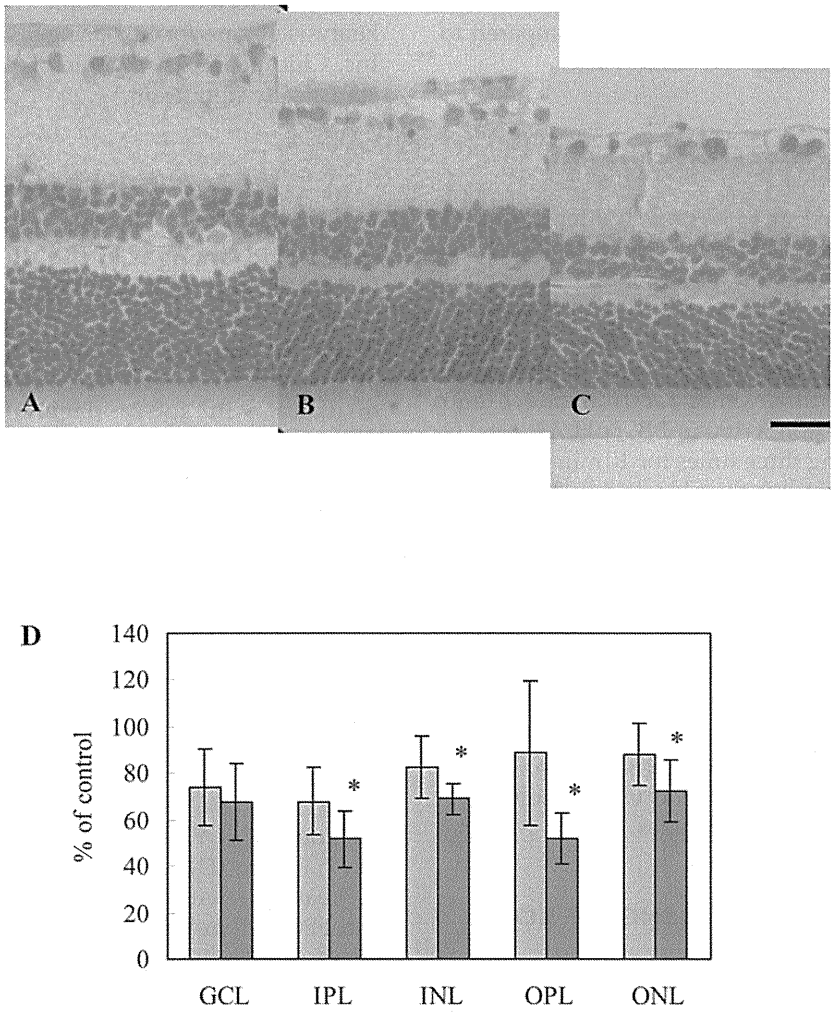

FIGURE 1 Light micrographs of a cross-section through normal rat retina (A) and at 7 days after ischemia when treated with control class-matched mAb (anti-*Keyhole Limpet* hemocyanin mAb, IgG2a) (B) or anti-HMGB1 mAb (C). Percentages indicate change relative to control values for the number of GCL cells and for the IPL, INL, ONL, and OPL thicknesses 7 days after ischemia when treated with IgG2a (▒) or anti-HMGB1 (■). Results are expressed as the mean ± SD (*$p < 0.05$). Scale bar = 20 μm.

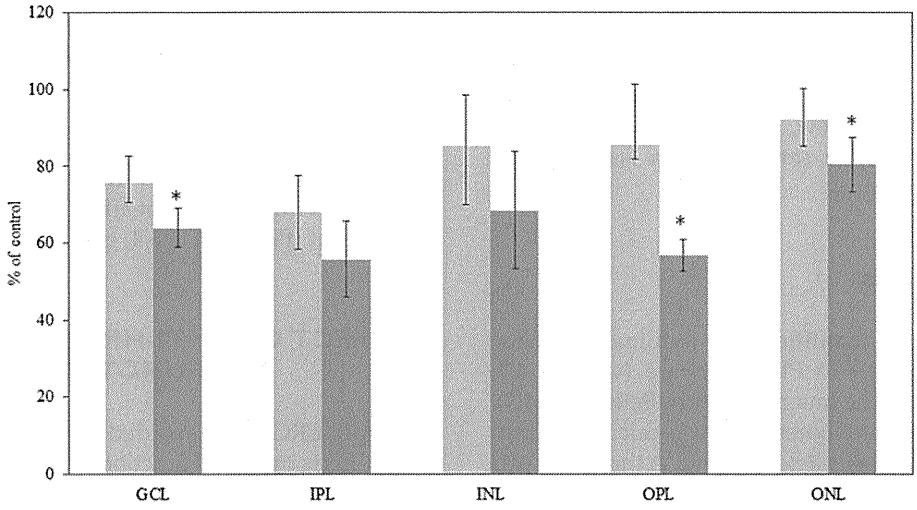

FIGURE 2 Percentages indicate change relative to control values for the number of RGC cells and for IPL, INL, ONL, and OPL thickness 7 days after ischemia when treated with intravenous injections of IgG2a (▒) or anti-HMGB1 (■). Results are expressed as the mean ± SD (*$p < 0.05$).

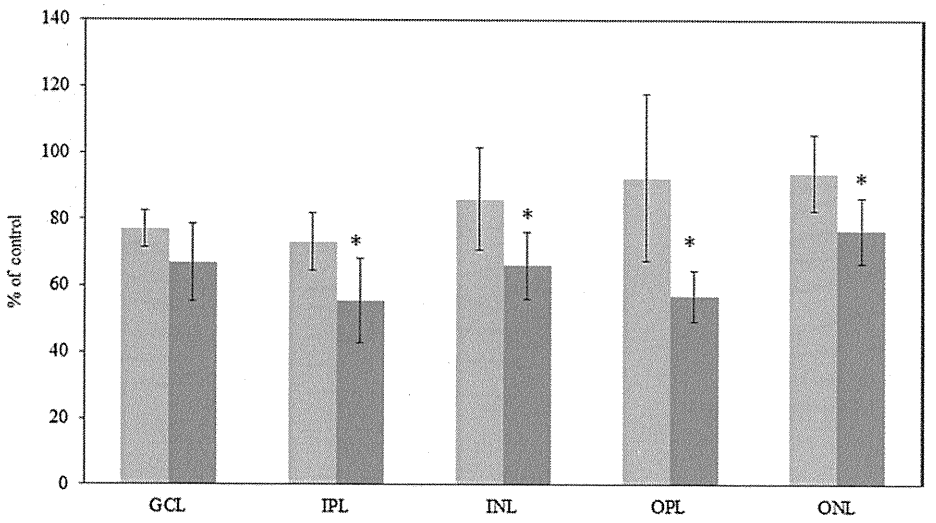

FIGURE 3 Percentages indicate change relative to control values for the number of RGC cells and for IPL, INL, ONL, and OPL thickness 7 days after ischemia when treated local administration of IgG2a (▒) or anti-HMGB1 (■). Results are expressed as the mean ± SD (*$p < 0.05$).

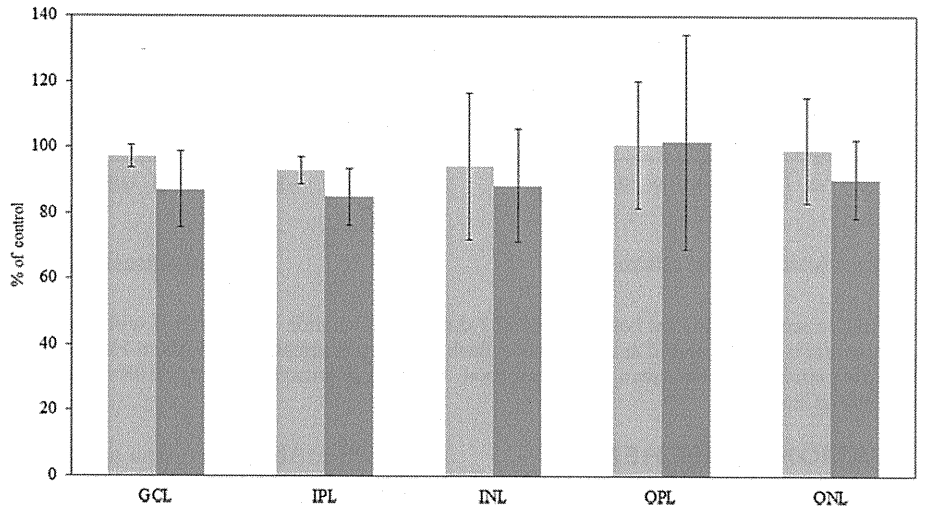

FIGURE 4 Percentages indicate change relative to control values for the number of RGC cells and for IPL, INL, ONL, and OPL thickness 7 days after treatment with IgG2a (▒) or anti-HMGB1 (■). Results are expressed as the mean ± SD.

Scotopic ERG was measured 7 days after the intraperitoneal injection of anti-HMGB1 mAb. There was no significant difference between the two groups (Figure 6A, B) ($n=5$, each group). Treatment with anti-HMGB1 did not affect the retinal function in normal rat.

IMMUNOHISTOCHEMISTRY

We examined the expression of HMGB1 in the retina at 6, 12, and 24 h after 45 min of ischemia (Figure 7). Figure 3A shows the localization of HMGB1 in the normal retina. Immunostaining for HMGB1 was noted in the ONL in the normal retina. However, immunostaining for HMGB1 in the post-ischemic retina (Figure 7B–D) was detected in not only the ONL but also in the INL and GCL. A high degree of edema was noted in the post-ischemic retina.

We examined the effect of anti-HMGB1 mAb on endogenous HMGB1 expression in the normal retina and the retina at 6, 12, and 24 h after 45 min of ischemia (Figure 8). Intraperitoneal injection of anti-HMGB1 mAb was administered 30 min before ischemia. Normal eye balls were enucleated after 30 min administration of anti-HMGB1. Administration of anti-HMGB1 suppressed the expression of endogenous HMGB1.

We also examined the direct effect of anti-HMGB1 mAb on retinal HMBG1 expression (Figure 9). Normal eye balls were enucleated at 12 h after intravitreous injection of anti-HMGB1. Immunostaining for HMGB1 was not detected.

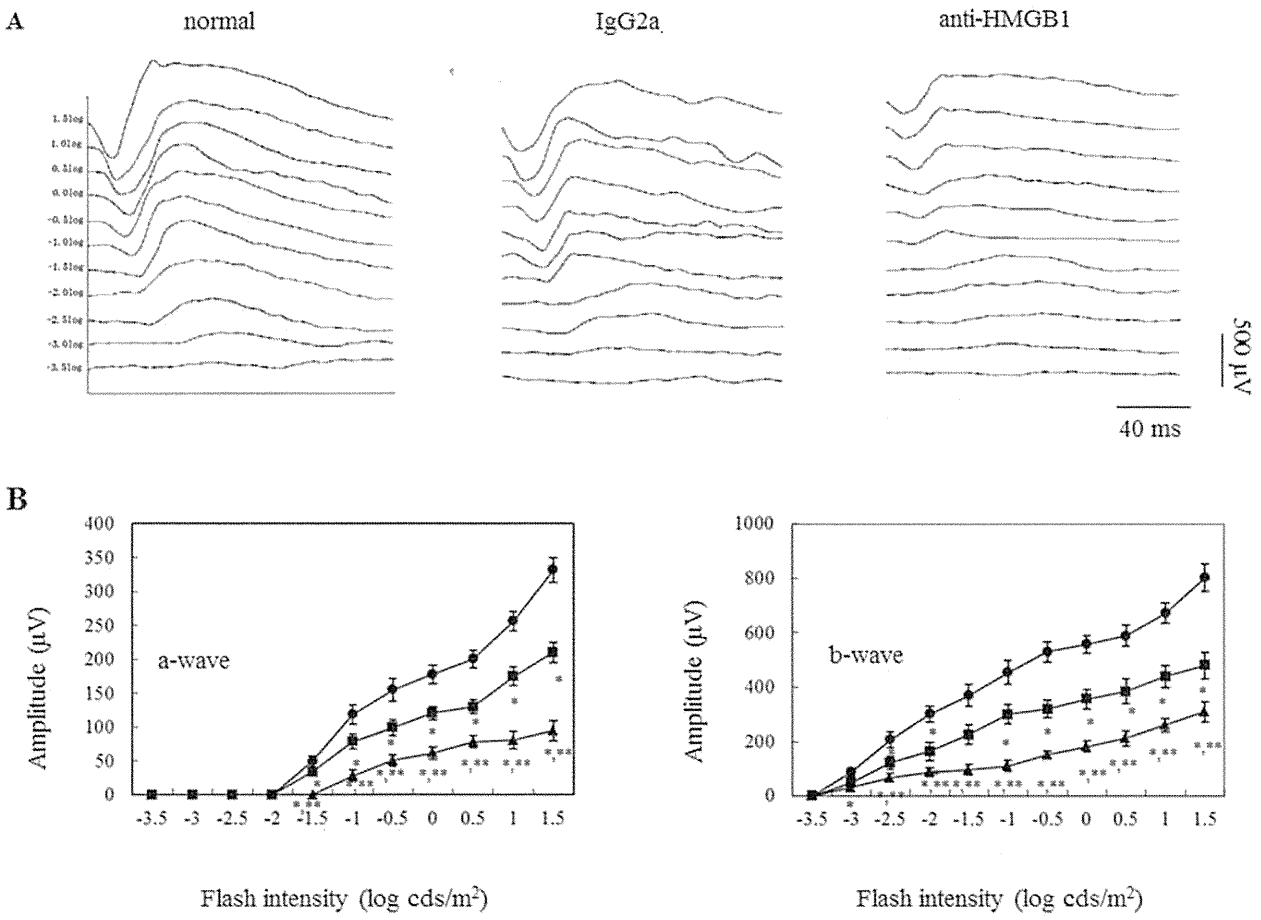

FIGURE 5 (A) Representative scotopic ERGs at baseline and at 7 days after ischemia when treated with control mAb or anti-HMGB1 mAb. (B) Amplitudes for a- and b-waves plotted as a function of flash intensity. Pretreatment with anti-HMGB1 mAb markedly reduced the amplitudes. Results are expressed as the mean ± SD. •: normal, ▪: IgG2a, ▲: anti-HMGB1. *$p<0.05$ versus normal retina. **$p<0.05$ versus ischemic retina with IgG2a.

ROS ACTIVATION BY ISCHEMIA

We used DHE staining to test whether ROS were enhanced by treatment with 200 μg anti-HMGB1 mAb. DHE specifically reacts with intracellular O_2^-, a ROS, and is converted to the red fluorescent compound ethidium in nuclei. In the post-ischemic retina, DHE fluorescence was clearly up-regulated in the retinal neuronal cells, and this up-regulation was efficiently enhanced by anti-HMGB1 mAb (Figure 10A–C). Figure 9D shows the quantified specific retinal DHE fluorescence. The mean ROS activation was significantly increased by treatment with anti-HMGB1 mAb ($n=4$, each group).

DISCUSSION

This study shows that, compared to the IgG2a treatment, pretreatment with anti-HMGB1 mAb significantly enhanced the ischemic injury of the retina. The results also showed that there was expression of HMGB1 mAb in the retina after ischemia-reperfusion injury.

A recent study showed that HMGB1 inhibited glial glutamate transport by GLAST in mouse gliosomes and suggested that HMGB1 can increase extracellular glutamate levels in ischemic brain.[21] We previously reported that anti-HMGB1 mAb suppressed ischemia-reperfusion-induced brain injury in a transient middle cerebral artery occlusion model in rats.[17] Based on these findings, we predicted that neutralizing mAb could be used to inhibit HMGB1 activity, and thus to significantly decrease the progression of the retinal ischemia-reperfusion injury. However, use of the neutralizing anti-HMGB1 mAb treatment in the present study remarkably increased the retinal damage following ischemia-reperfusion. This was due to an increased production of ROS caused by the anti-HMGB1 mAb treatment. Therefore, it might be possible that elevated levels of HMGB1 had neuroprotective effects against retinal ischemia- reperfusion injury. It has also been reported that treatment with anti-HMGB1 mAb increased ischemia-reperfusion

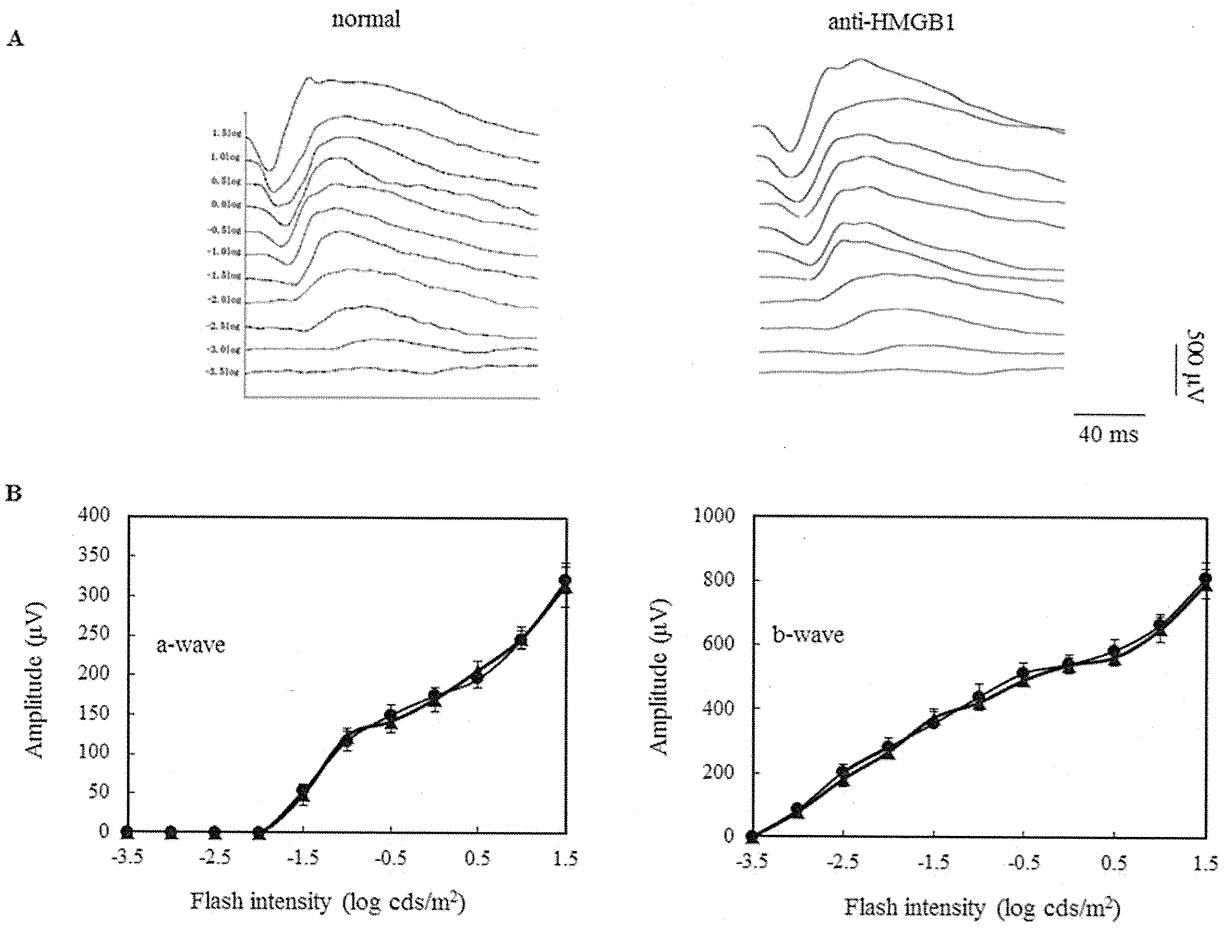

FIGURE 6 (A) Representative scotopic ERGs 7 days after treatment with anti-HMGB1. (B) Amplitudes for a- and b-waves plotted as a function of flash intensity. Results are expressed as the mean ± SD. •: normal, ▲: anti-HMGB1.

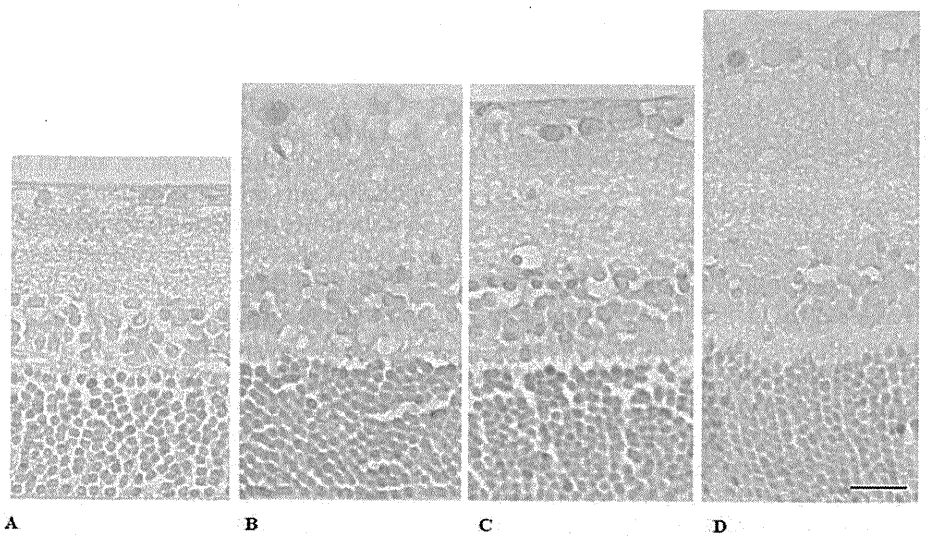

FIGURE 7 Immunohistochemical staining of HMGB1 expression in the retina. Retinal sections from normal animals (A) or 6h (B), 12h (C), or 24h (D) after ischemia. Scale bar = 20 μm.

injury in the rat heart.[22] Therefore, it appears that the effect of anti-HMGB-1 mAb depends on the organ involved.

When the IOP is increased, glutamate is released from the retina during and after the ischemia.[3,23,24] The major causes of the cell death that occur after activation

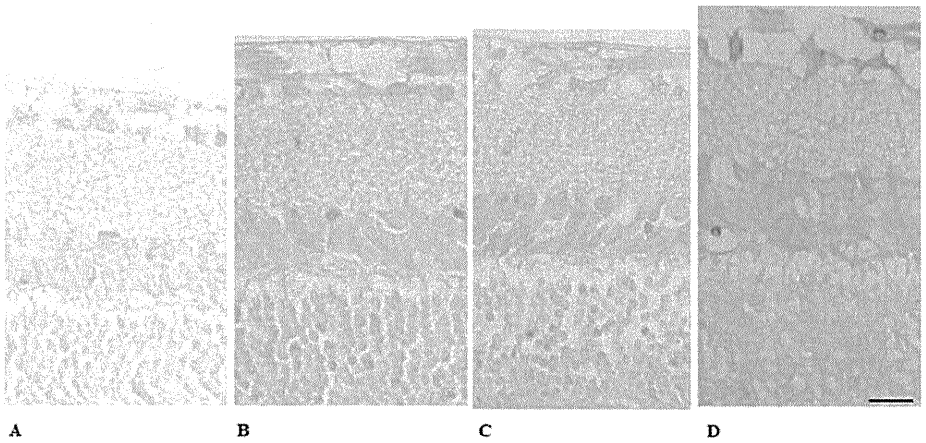

FIGURE 8 The effect of anti-HMGB1 mAb on endogenous HMGB1 expression. Intraperitoneal injection of anti-HMGB1 mAb was administered 30 min before ischemia. Retinal sections from normal animals (A) or 6 h (B), 12 h (C), or 24 h (D) after ischemia. Scale bar = 20 μm.

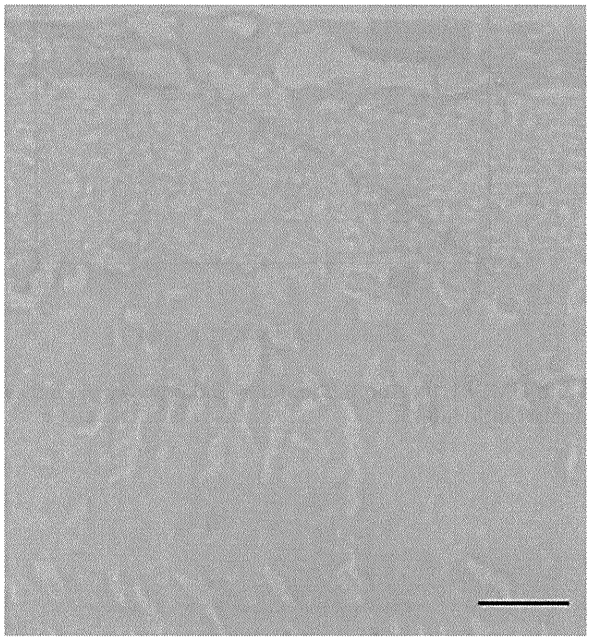

FIGURE 9 The direct effect of anti-HMGB1 mAb on endogenous HMGB1 expression in the normal retina. Scale bar = 20 μm.

of the *N*-methyl-D-aspartate (NMDA) subtype of glutamate receptors are related to the influx of calcium into the cells and the generation of free radicals.[25] Excessive accumulation of intracellular free Ca^{2+} ($[Ca^{2+}]_i$) can have a wide range of detrimental effects, including inhibition of mitochondrial function, reduction of cellular ATP levels, enhancement of ROS production, and activation of cellular proteases and nitric oxide (NO) synthase.[26] Since production of ROS was increased by anti-HMGB1 mAb treatment in the current study, anti-HMGB1 mAb played a large deleterious role in the resultant ischemia-reperfusion injury. In the present study, there was an increase in the HMGB1 level in the retina after the ischemia-reperfusion injury. These results suggest that endogenous HMGB1 released from retinal cells may modulate ischemia-reperfusion injury in the retina. Therefore, the anti-HMGB1 mAb treatment increased the delayed neuronal death.

We evaluated the functional retinal damage after ischemia-reperfusion injury by measuring the ERG a- and b-wave amplitudes. The b-wave of the ERG has been identified as a particularly sensitive index of retinal ischemia both in humans[25] and in experimental models of retinal ischemia in vitro.[27] After the anti-HMGB1 mAb treatment, there was a decrease in the thickness of ONL following ischemia-reperfusion, with the a-wave of the ERG also lower than that noted in the eyes treated with IgG2a. There was a good correlation between the ERG for both a- and b-waves and the histological results. It has been reported that administration of pentobarbital enhance the a- and b-wave of the ERG.[28,29] Under the anesthesia, many factors indirectly affecting the retinal activity could not be completely excluded.

It has been reported in previous studies that HMGB1 is expressed in GCL, INL, ONL, the inner and outer segments of photoreceptors, and in the retinal pigment epithelial cells in normal retina.[30,31] However, the current immunohistochemical study showed that HMGB1 was present in the ONL in normal retinas, which may be due to the use of different antibodies in the various studies (monoclonal antibody vs. polyclonal antibody).

HMGB1 passively released from necrotic cells.[32] Cell death was frequently observed in both the GCL and the INL after 3 h of ischemia-reperfusion.[33] In the present study, we demonstrated that immunostaining for HMGB1 in the post-ischemic retina was detected in not only the ONL but also in the INL and GCL. HMGB1 may play a key role in the protection of retinal injury after ischemia-reperfusion.

The current study showed, for the first time, that treatment with anti-HMGB1 mAb increased ischemia-reperfusion injury in the rat retina. Further investigations are needed to clarify the mechanism of anti-HMGB1 mAb in retinal ischemia-reperfusion

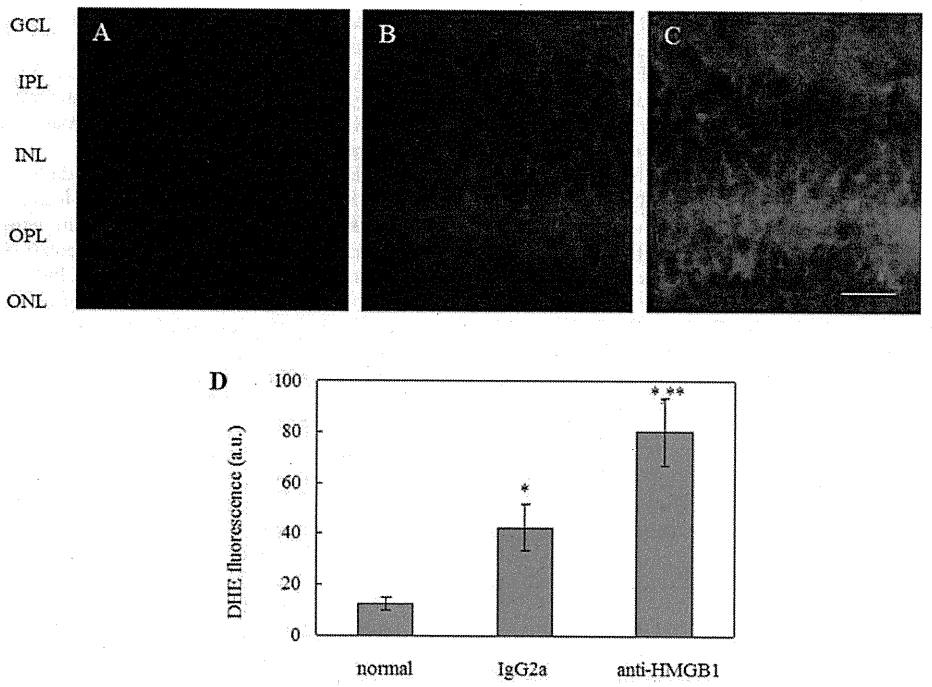

FIGURE 10 Effect of anti-HMGB1 mAb pretreatment on the release of ROS. The use of DHE to detect ROS indicated up-regulation of retinal neuronal cells in the retina after ischemia (IgG2a (B) as compared to normal retina (A)). Pretreatment with anti-HMGB1 mAb enhanced the level of ROS (C). (D) Quantified specific retinal DHE fluorescence is expressed for sections in arbitrary units (AU) for each group. Data express the mean ± SD; $*p < 0.05$ normal retina. $**p < 0.05$ versus ischemic retina with IgG2a. Scale bar = 20 μm.

injury. Additionally, anti-HMGB1 mAb function needs be further explored, as this could potentially lead to the development of neuroprotective therapeutic strategies for acute retinal ischemic disorders.

ACKNOWLEDGMENTS

This work was supported by a Grant-in-Aid for Scientific Research from The Ministry of Education, Culture, Sports, Science, and Technology of Japan (20592078).

Declaration of interest: The authors report no conflicts of interest. The authors alone are responsible for the content and writing of the paper.

REFERENCES

[1] Tsujikawa A, Ogura Y, Hiroshiba N, Miyamoto K, Kiryu J, Honda Y. Tacrolimus (FK506) attenuates leukocyte accumulation after transient retinal ischemia. *Stroke*. 1998;29:1431–1437; discussion 1437–1438.

[2] Tsujikawa A, Ogura Y, Hiroshiba N, Miyamoto K, Kiryu J, Tojo SJ, Miyasaka M, Honda Y. Retinal ischemia-reperfusion injury attenuated by blocking of adhesion molecules of vascular endothelium. *Invest Ophthalmol Vis Sci*. 1999;40:1183–1190.

[3] Hirooka K, Miyamoto O, Jinming P, Du Y, Itano T, Baba T, Tokuda M, Shiraga F. Neuroprotective effects of D-allose against retinal ischemia-reperfusion injury. *Invest Ophthalmol Vis Sci*. 2006;47:1653–1657.

[4] Iwama D, Miyamoto K, Miyahara S, Tamura H, Tsujikawa A, Yamashiro K, Kiryu J, Yoshimura N. Neuroprotective effect of cilostazol against retinal ischemic damage via inhibition of leukocyte-endothelial cell interactions. *J Thromb Haemost*. 2007;5:818–825.

[5] Sakamoto K, Kawakami T, Shimada M, Yamaguchi A, Kuwagata M, Saito M, Nakahara T, Ishii K. Histological protection by cilnidipine, a dual L/N-type $Ca^{(2+)}$ channel blocker, against neurotoxicity induced by ischemia-reperfusion in rat retina. *Exp Eye Res*. 2009;88:974–982.

[6] Büchi ER. Cell death in the rat retina after a pressure-induced ischemia-reperfusion insult: An electron microscopic study. I: Ganglion cell layer and inner nuclear layer. *Exp Eye Res*. 1992;55:605–613.

[7] Nitatori T, Sato N, Waguri S, Karasawa Y, Araki H, Shibanai K, Kominami E, Uchiyama Y. Delayed neuronal death in the CA1 pyramidal cell layer of the gerbil hippocampus following transient ischemia is apoptosis. *J Neurosci*. 1995;15:1001–1011.

[8] Rosenbaum DM, Rosenbaum PS, Gupta A, Michaelson MD, Hall DH, Kessler JA. Retinal ischemia leads to apoptosis which is ameliorated by aurintricarboxylic acid. *Vision Res*. 1997;37:3445–3451.

[9] Halliwell B, Gutteridge JM. Free Radicals in Biology and Medicine. Oxford, UK: Clarendon Press; 1985.

[10] Goodwin GH, Sanders C, Johns EW. A new group of chromatin-associated proteins with a high content of acidic and basic amino acids. *Eur J Biochem*. 1973;38:14–19.

[11] Lotze MT, Tracey KJ. High-mobility group box 1 protein (HMGB1): Nuclear weapon in the immune arsenal. *Nat Rev Immunol*. 2005;5:331–342.

[12] Calogero S, Grassi F, Aguzzi A, Voigtländer T, Ferrier P, Ferrari S, Bianchi ME. The lack of chromosomal protein Hmgb1 does not disrupt cell growth but causes lethal hypoglycaemia in newborn mice. *Nat Genet*. 1999;22:276–280.